

## Accepted Manuscript

Title: Nanoscale Pt Thin Film Sensor for Accurate Detection of ppm Level Hydrogen in Air at High Humidity

Authors: Takahisa Tanaka, Shinsuke Hoshino, Tsunaki Takahashi, Ken Uchida



PII: S0925-4005(17)32246-3  
DOI: <https://doi.org/10.1016/j.snb.2017.11.115>  
Reference: SNB 23609

To appear in: *Sensors and Actuators B*

Received date: 28-6-2017  
Revised date: 15-11-2017  
Accepted date: 20-11-2017

Please cite this article as: Takahisa Tanaka, Shinsuke Hoshino, Tsunaki Takahashi, Ken Uchida, Nanoscale Pt Thin Film Sensor for Accurate Detection of ppm Level Hydrogen in Air at High Humidity, *Sensors and Actuators B: Chemical* <https://doi.org/10.1016/j.snb.2017.11.115>

This is a PDF file of an unedited manuscript that has been accepted for publication. As a service to our customers we are providing this early version of the manuscript. The manuscript will undergo copyediting, typesetting, and review of the resulting proof before it is published in its final form. Please note that during the production process errors may be discovered which could affect the content, and all legal disclaimers that apply to the journal pertain.

# Nanoscale Pt Thin Film Sensor for Accurate Detection of ppm Level Hydrogen in Air at High Humidity

*Takahisa Tanaka<sup>a</sup>, Shinsuke Hoshino<sup>a</sup>, Tsunaki Takahashi<sup>a</sup>, Ken Uchida<sup>a\*</sup>*

\*corresponding author

<sup>a</sup>Department of Electronics and Electrical Engineering, Faculty of Science and Technology, Keio University, 3-14-1, Hiyoshi, Yokohama 223-8522, Japan

E-mail of corresponding author: uchidak@elec.keio.ac.jp

## Highlights

- Sub-ppm level hydrogen sensing with humidity robustness was achieved using platinum nanoscale film.
- The sensor resistance changes linearly as a function of hydrogen concentration.
- Effects of adsorbate were thoroughly investigated by carefully controlling the components and concentrations of the ambient.
- Not only hydrogen concentration but also time dependence of the sensor was accurately modeled, based on kinetics of gases.

**ABSTRACT** Hydrogen is an important biomarker for the human digestive system. However, accurate detection of ppm-level hydrogen in breath is difficult due to the competing detection of high concentration water. We fabricated Pt thin films that respond to hydrogen in air at concentrations as low as 500 ppb. In both dry and humid air, these films have almost identical response to hydrogen, i.e., their resistance decreases linearly with increasing hydrogen concentration regardless of relative humidity. Even at high relative humidity, these Pt thin films can detect ppm-level hydrogen. Furthermore, it was strongly suggested that these Pt thin films responded to low-level hydrogen in air expired by a healthy human. Based on the chemical kinetics, namely the adsorption and desorption of hydrogen and oxygen, the sensor response is quantitatively described by relating the hydrogen surface coverage to the magnitude of electron scattering at the Pt surface. The proposed model successfully reproduces the effects of hydrogen concentration and time on the sensor response, particularly at hydrogen concentrations below 20 ppm. Based on this model, these Pt thin film sensors have the potential to detect 1 ppm hydrogen in expired air within 30 s.

**Keywords:** Platinum; hydrogen; adsorption; humidity; scattering; sensor

## 1. Introduction

Hydrogen in expired air can be an important biomarker for the condition of the human digestive system [1–3]. Expired air contains hydrogen in the ppm range [1–3] and is nearly saturated with water vapor. The sensor used to measure the hydrogen content of expired air should show high sensor response for hydrogen and robustness against humidity at the same time. Many kinds of sensors have been proposed for hydrogen sensing, such as nanostructured metal resistors [4–11], metal–oxide semiconductor field-effect transistors (MOSFETs) [12–16], and graphene-based materials [17–23]. Pd and Pt have attracted much attention for use in nanostructured metal resistors, because of their high reactivity with hydrogen [4–11]. Unfortunately, Pd-based hydrogen sensors are strongly affected by humidity [18,24]. On the one hand, reported Pt-based sensors were mainly evaluated in dry air or nitrogen atmosphere [8,9,11], and their robustness against humidity has not been fully characterized. Furthermore, a quantitative explanation of the hydrogen sensing mechanisms has not been reported. At the qualitative level, the experimentally obtained sensor response of nanostructured Pt resistors for hydrogen sensing can be described as follows [5,11]. In room air, the Pt surface is almost completely covered by adsorbed oxygen atoms. Hydrogen in the air replaces the adsorbed oxygen on the surface. The amount and species of the adsorbates affect the scattering of conduction electrons at the metal surface. By being a weaker scattering source than oxygen atoms, the adsorbed hydrogen atoms change the film conductivity. This model can successfully explain the qualitative decrease in the resistance of Pt nanostructures in a hydrogen-containing atmosphere. However, the actual resistance change in these sensors cannot be determined a priori. To design hydrogen sensors suitable for use with expired air, a quantitative model is required to assess their robustness against humidity and sensor response.

In this study, we experimentally evaluated the sensor response of Pt thin film hydrogen sensors in dry, humid and expired air by changes in their resistance, and clarified the sensing mechanism based on the underlying chemical kinetics. The experimental results indicate that these sensors are adequate for hydrogen detection in expired air, which has high relative humidity and ppm-range hydrogen. Then, we used the hydrogen and oxygen adsorption/desorption kinetics on the Pt surface to quantitatively model the sensor response of the Pt thin films, based on the surface hydrogen coverage ratio. The proposed model could successfully assess the robustness against humidity and sensor response of the Pt thin film sensors, and these Pt thin films have satisfactory performance for hydrogen sensing in expired air.

## **2. Experimental method**

### **2.1. Sensor Fabrication**

Pt thin films were deposited on silicon substrates with 300-nm-thick silicon dioxide ( $\text{SiO}_2$ ) layers by electron beam deposition. The deposition rate of 0.02 nm/s and film thickness of 5 nm were confirmed by a quartz oscillator. The aluminum electrodes were also fabricated by electron beam deposition. The deposition rate and thickness of the electrodes were 0.2 nm/s and 100 nm, respectively.

### **2.2. Characterization of Sensor**

Surface morphology of Pt thin films was observed by an atomic force microscope (AFM, Shimadzu SPM-9700). Then, Cross sectional images of Pt thin films were characterized by a transmission electron microscope (TEM, Hitachi H-9000NAR) with an acceleration energy of 300 kV. For the evaluation of surface orientation, high resolution TEM images and nano-beam diffraction (NBD) were taken by TEM (JEOL JEM-ARM200F) with an acceleration energy of 200 kV and a beam spot of 1 nm.

### 2.3. Hydrogen Sensing by Exposure to Gas Flow

Pt thin films were heated by an external heater and exposed to a gas of given composition at a flow rate of 500 sccm. To obtain the sensor response, the electric current was measured under a constant bias voltage of 1.0 V during the hydrogen sensing with a Keithley2636 instrument.

### 2.4. Hydrogen Sensing by Exposure to Expired Air

Pt thin films were heated by an external heater and exposed to air expired by a healthy human. Except for exposing to an expired air, Pt thin films were exposed to an open air. After examinee ingested two rice balls and 0.5 L of milk as lunch, sensing of hydrogen in air expired by the examinee was performed every 30 minutes. In each sensing measurement, the sensor was under expired air for 30 seconds. To obtain the sensor response to hydrogen, the electric current of the sensor under the expired air was measured using Keithley 2636 instrument at a constant bias voltage of 1.0 V.

### 2.5. Hydrogen Sensing by Controlling Ambience

Pt thin films were set in the prober that was isolated from room air. The air in the prober was substituted by the target gas with the flow rate of 1000 sccm. The hydrogen gas concentration at the Pt thin films was numerically simulated by the COMSOL Multiphysics software. To obtain the sensor response, the electric current was also measured under a constant bias voltage of 1.0 V by a Keithley2636 instrument during the hydrogen sensing.

### 2.6. DFT Simulations

DFT simulations were performed by Quantum Espresso [25] software with PW91 ultra-soft pseudo potential [26]. The Monkhorst-Pack mesh of  $32 \times 32 \times 1$ , cut-off energy of 30 Ry, and Gaussian smearing of 0.05 Ry were employed in our calculations. For the Pt thin films, we assumed five Pt atomic layers with the surface orientation of (100). The positions of the top two

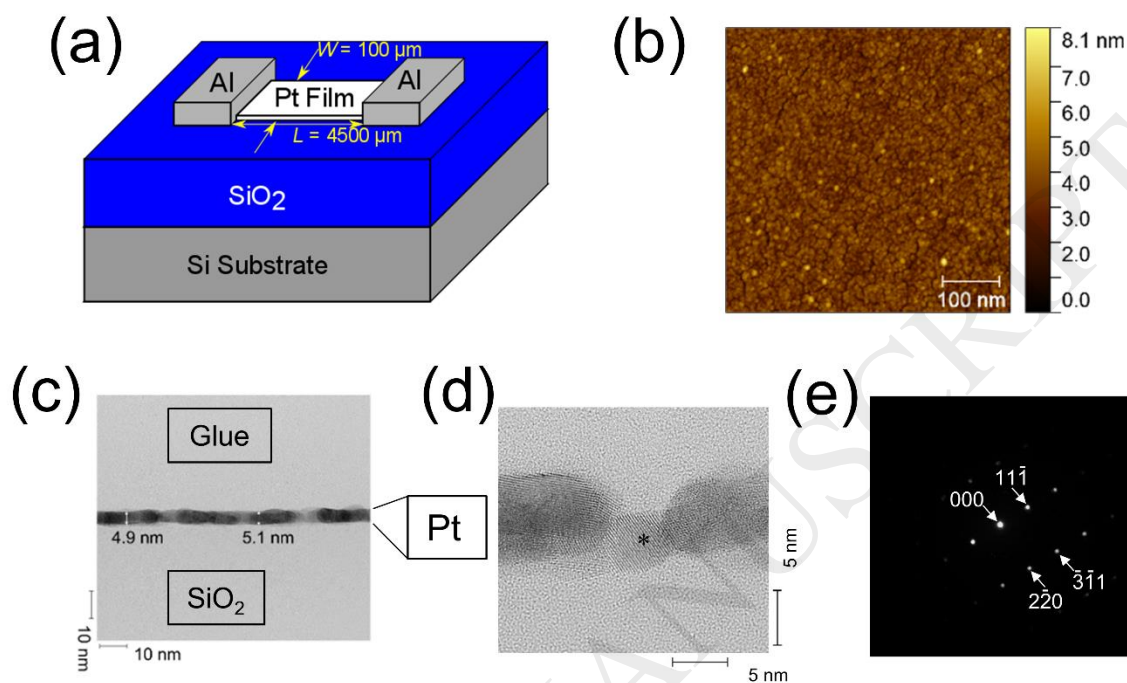
Pt layers and the adsorbates were optimized by the relaxation calculation, while the positions of the bottom three Pt layers were fixed [27].

### 2.7. Surface Coverage Simulations

Numerical simulations of surface coverage were performed by solving the chemical kinetic equation in an explicit method. First-order adsorption and desorption were assumed for both oxygen and hydrogen [28]. In our experiments, the Pt surface was exposed to the target gas flow or composition-controlled ambience. Therefore, the composition of the gas phase was fixed in our calculations.

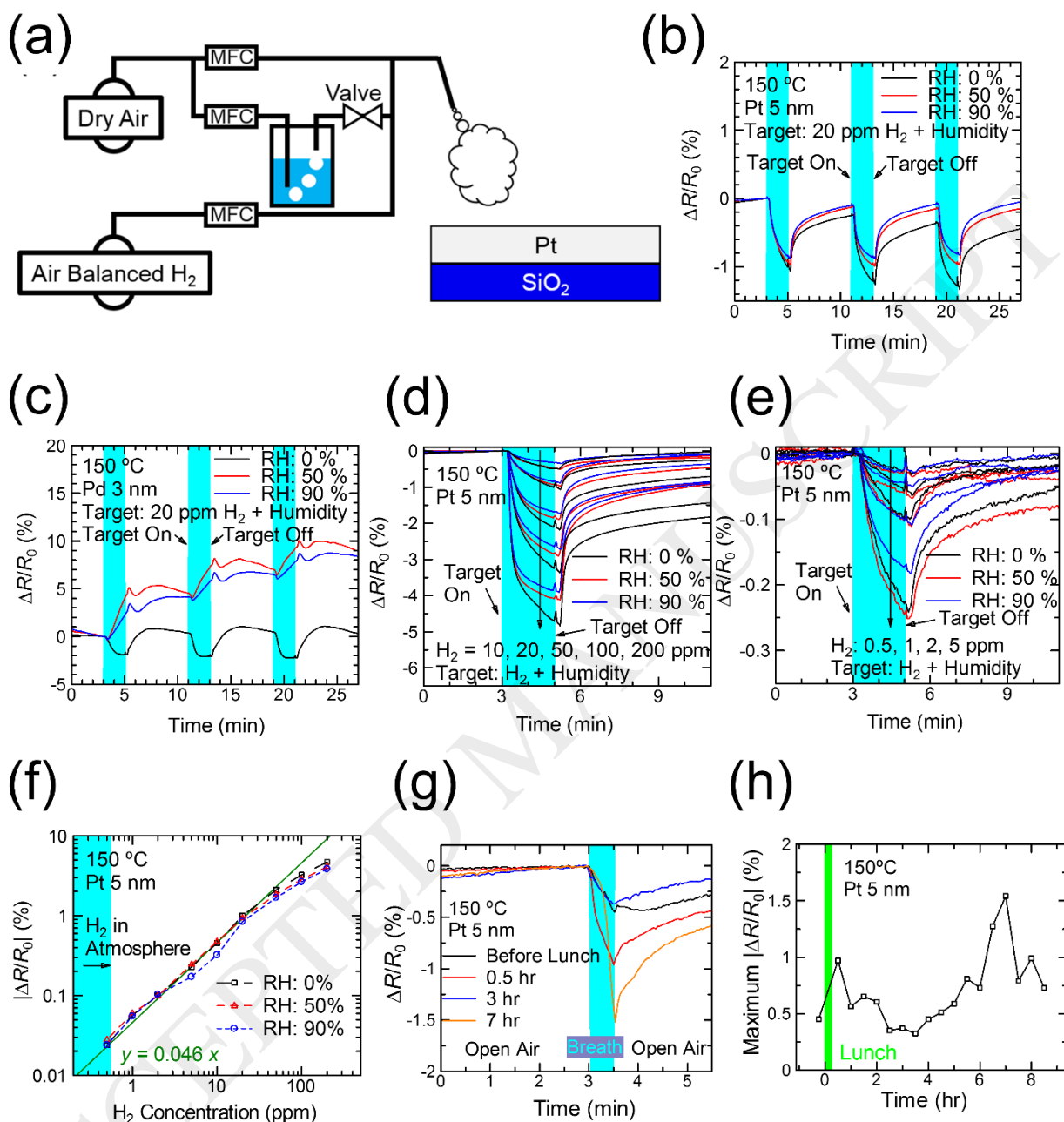
## 3. Result and discussion

Fig. 1a shows the schematic diagram of the sensor structure. The 300-nm-thick  $\text{SiO}_2$  layer electrically insulates the Pt thin film from the Si substrate. Fig. 1b and 1c show the surface morphology and cross sectional image of the Pt thin films, respectively. Polycrystalline Pt films with cracks were observed. Fig. 1d shows the high resolution TEM image of the Pt thin film. The typical grain size of Pt is ranging from 5 to 10 nm. Fig. 1e shows the nano-beam diffraction pattern obtained by the point indicated in Fig. 1d. From the diffraction pattern, surface orientations of Pt(111), Pt(110) and Pt(311) were derived. Therefore, fabricated Pt thin film has similar surface orientations to previously reported Pt surface [29]. The setup for hydrogen sensing with these structures is schematically shown in Fig. 2a. By changing the flow rates through the mass flow controllers (MFCs), the concentration of hydrogen and relative humidity (RH) were controlled. Assuming an initial resistance of  $R_0$ , the sensor response is determined as the ratio between the resistance change  $\Delta R$  and  $R_0$ .



**Fig. 1.** (a) Schematic diagram of the Pt hydrogen sensor. The Al pads act as electrodes. (b) Tomography obtained by AFM. (c) Cross-sectional image of the film taken by TEM. The thickness of the polycrystalline Pt layer was measured as 5 nm. (d) High resolution image of TEM. The asterisk (\*) means the position where nano-beam diffraction analysis was performed. (e) Diffraction pattern obtained from nano-beam diffraction with indications of surface orientations.





**Fig. 2.** (a) Schematic diagram of the hydrogen sensing setup. By bubbling dry air in water, the humidity of the target gas is controlled. The mixture of dry, wet, and hydrogen-containing air was sprayed onto the hydrogen sensor. MFC: mass flow controller. (b) Sensor response of Pt thin film sensor obtained by spraying air containing 20 ppm hydrogen at different RH (determined at 27 °C). The cyan regions (3–5, 11–13, and 19–21 min) represent the duration in which target gas was

sprayed onto the sensor, while dry air was sprayed during the rest of the time. (c) Sensor response of Pd thin film obtained under the same condition as (b). Dynamic current response and recovery plots for H<sub>2</sub> concentration of (d) 10–200 ppm and (e) 0.5–5 ppm. (f) Hydrogen concentration dependence of sensor response in Pt thin film sensor. The green solid line of  $y = 0.046 x$  is artificially inserted to show the linearity of the relationship. Here, the boundary between the cyan and white regions represents the hydrogen concentration in room air. (g) Dynamic current response and recovery plots for an expired air. Times indicated as legends mean transit time after the starting time of the lunch. (h) Time dependence of maximum sensor response. The maximum value of sensor response during each 30-second time duration under an expired air at each time. The measurements were performed before and after lunch.

The sensor response of the Pt thin film was found to be robust against humidity, as shown in Fig. 2b. The film was heated at 150 °C, while the target gas was at room temperature. The humidity only had a weak effect on the hydrogen sensing when the RH was increased from 0% to 90%. Compared to these Pt thin films, Pd thin films are much less robust as hydrogen sensors. Fig. 2c shows the hydrogen sensing performance of a Pd thin film at 150 °C. In the absence of humidity, the resistance of the Pd film decreases in the presence of hydrogen, because of the elongated conduction path originating from the volume increase caused by Pd hydrogenation. However, at RH = 50–90 % and a gas temperature of 27 °C, the response is inverted. This effect of humidity could be attributed to the consumption of adsorbed hydrogen to form water with the hydroxyl originating from the adsorbed water [24]. This result indicates that the nanostructured Pd resistor is not suitable for hydrogen detection in humid air. Hereon, we concentrate on the measurements and modeling of hydrogen sensing by the Pt thin films. For hydrogen concentrations ranging from 500 ppb to 200 ppm, the sensor response of the Pt thin film was measured under RH = 0, 50, and 90 % at the gas temperature of 27 °C as shown in Fig. 2d and 2e. From these measurements, the same linear sensor response relation independent of RH was obtained as shown in Fig. 2f. Since room air typically contains 550 ppb hydrogen [30], expired air should contain more hydrogen than that. Thus, the response of the Pt thin films tested here indicates sufficient sensor response for hydrogen detection in expired air. Furthermore, sensor response under expired air are shown as Fig. 2g and 2h. Apparent increases of sensor response just after the lunch and 7 hours later since the starting time of lunch were observed. These increases of sensor response would be correlated to an increase in hydrogen in breath after examinee's ingesting foods; it is known that hydrogen concentration is increased approximately 6 hours later since food was taken by examinees [31–

33]. Therefore, this experiment strongly suggested that the Pt thin film sensor responded to low-level hydrogen in air expired by a healthy human.

Fig. 3a shows the partial density of states attributed to the adsorbate obtained by DFT calculations. The additional density of states by adsorption induces surface scattering [34,35], which is the mechanism of hydrogen sensing in Pt thin films. The higher partial density of states caused by the adsorbed oxygen atom induces stronger surface scattering. The effect of adsorbate-induced surface scattering on the resistivity is represented as follows [34,35],

$$\frac{\Delta R}{R_{0,c}} = \frac{3}{16} \frac{\lambda_{Pt}}{t_{Pt}} (1 - p), \quad (1)$$

where  $R_{0,c}$  is the resistance of Pt without any adsorbates,  $\lambda_{Pt}$  is the mean free path of conduction electrons, and  $t_{Pt}$  is the thickness of the Pt film;  $p$  is an empirical parameter that depends on the specularity of surface scattering:  $p = 1$  represents completely specular scattering at the Pt surface, while  $p = 0$  represents completely diffusive scattering. As suggested in Fig. 3a, the oxygen-covered Pt surface has a small  $p$  value, while the hydrogen-covered one has a large  $p$  value. Therefore, we consider the amount of adsorbed hydrogen and oxygen atoms on the Pt surface at equilibrium:

$$\frac{d\theta_H}{dt} = 0 = S_{H_2} F_{H_2} \theta_{Pt} - k_{dH} \theta_H, \quad (2)$$

$$\frac{d\theta_O}{dt} = 0 = S_{O_2} F_{O_2} \theta_{Pt} - k_{dO} \theta_O, \quad (3)$$

$$\frac{d\theta_{H_2O}}{dt} = 0 = S_{H_2O} F_{H_2O} \theta_{Pt} - k_{dH_2O} \theta_{H_2O}, \quad (4)$$

where  $S_{H_2}/S_{O_2}/S_{H_2O}$  is the sticking coefficient of hydrogen/oxygen/water,  $F_{H_2}/F_{O_2}/F_{H_2O}$  is the respective surface impingement rate [36],  $k_{dH}/k_{dO}/k_{dH_2O}$  is the desorption rate coefficient of hydrogen/oxygen/water,  $\theta_H/\theta_O/\theta_{H_2O}$  is the surface coverage ratio, and  $\theta_{Pt}$  is the ratio of metal

surface without adsorbates. The employed values of the sticking coefficients, pre-exponential factor, and activation energy for desorption are listed in Table 1. Unless otherwise indicated, dry ambient ( $0 = \theta_{\text{H}_2\text{O}} = F_{\text{H}_2\text{O}}$ ) was assumed in our calculation. Nitrogen coverage on the surface was neglected. Fig. 3b shows the calculated Pt surface coverage by oxygen and hydrogen at different oxygen concentrations. When the Pt thin film is placed in room air ( $\text{H}_2 = 550$  ppb,  $\text{O}_2 = 20\%$ ), its surface is completely covered by oxygen atoms, and the adsorbed oxygen atoms change surface scattering from specular to diffusive. Because of the strong diffusive scattering at the initial Pt surface, eq. (1) is modified as follows,

$$\frac{\Delta R}{R_0} = -\frac{3}{16} \frac{\lambda_{\text{Pt}}}{t_{\text{Pt}}} p. \quad (5)$$

To derive eq. (5), we equate  $p$  to the hydrogen coverage ratio:  $p = 0$  for oxygen-covered Pt surface and  $p = 1$  for the hydrogen-covered one. In no oxygen ambient with hydrogen, oxygen atoms adsorbed on the Pt surface are completely substituted by hydrogen atoms, as shown in Fig. 3b. This change in the adsorbed species is responsible for the large decrease in resistance in Fig. 3c. The hydrogen concentration at the Pt thin film was numerically calculated by COMSOL Multiphysics package as shown in Fig. 3d. The large resistance decrease of around 12.6 % observed in Fig. 3c corresponds to  $\lambda_{\text{Pt}} = 3.4$  nm according to eq. (5). This  $\lambda_{\text{Pt}}$  value is in reasonable agreement with previously reported ones [5,37,38], indicating the validity of our assumptions. At the equilibrium condition, the changing surface coverage ratios by hydrogen and oxygen can explain the resistance change in the Pt thin films.

Next, we simulated the dependence of the sensor response on hydrogen concentration and time, by taking into account the time-dependent coverage change in eqs. (2) and (3). For equilibrium condition in humid air, saturated humidity in air (water of 3.5 vol%) was assumed in eq. (4), and

water coverage of Pt surface was taken into account. Fig. 4a demonstrates the good agreement of hydrogen concentration dependence between experiment and calculation at 150 °C. Furthermore, reasonable agreement of equilibrium sensor response between dry air and humid air accounts for a negligible water adsorption and the robustness against humidity. When the Pt surface is completely covered by hydrogen atoms, the resistance change of the Pt thin films becomes saturated (blue dash line). Hence, this model could be used to estimate the effect of the hydrogen concentration on the sensor response. The time-dependent sensor response at low hydrogen concentration below 20 ppm was also reproduced by our model, as shown in Fig. 4b and 4c. However, at high hydrogen concentrations, the calculated time dependence slightly deviates from experimental data as shown in Fig. 4c. Such deviation would be caused by catalytic water formation on the Pt surface. The calculated coverage change rates by oxygen desorption, hydrogen desorption, and water formation at different hydrogen concentrations are shown in Fig. 4d. The catalytic water formation is simplified from the previously reported OH-mediated two-step reaction [28,36], and a pre-exponential factor of  $4 \times 10^2 \text{ s}^{-1}$  and an activation energy of 13.4 kcal/mol were adopted. Although the former value contains much uncertainty, the qualitative result of Fig. 4d is not affected. At low hydrogen concentration below 20 ppm, the surface coverage change is dominated by oxygen desorption, as illustrated in Fig. 4e. Therefore, the sensor response is precisely predicted by adsorption and desorption of hydrogen and oxygen, in contrast to previous works in which catalytic water formation is caused by high temperature and high  $\text{H}_2$  concentration [28,36]. On the other hand, at high hydrogen concentrations, water formation also contributes the coverage change as illustrated in Fig. 4f, and the calculated time dependence slightly deviates from experimental data as shown in Fig. 4c. Therefore, the robustness against humidity in hydrogen sensing is attributed to the small contribution of water to the hydrogen surface coverage. Based on

our model, the  $|\Delta R/R_0|$  value after introducing 1 ppm hydrogen for 30 s is estimated to be 0.021 %. In comparison, the typical fluctuation of  $|\Delta R/R_0|$  for our Pt thin films is 0.004 %. From the time-dependent hydrogen and oxygen adsorption/desorption and experiments related to an expired air, we believe these Pt thin films could be applied to hydrogen sensing in actual expired air.

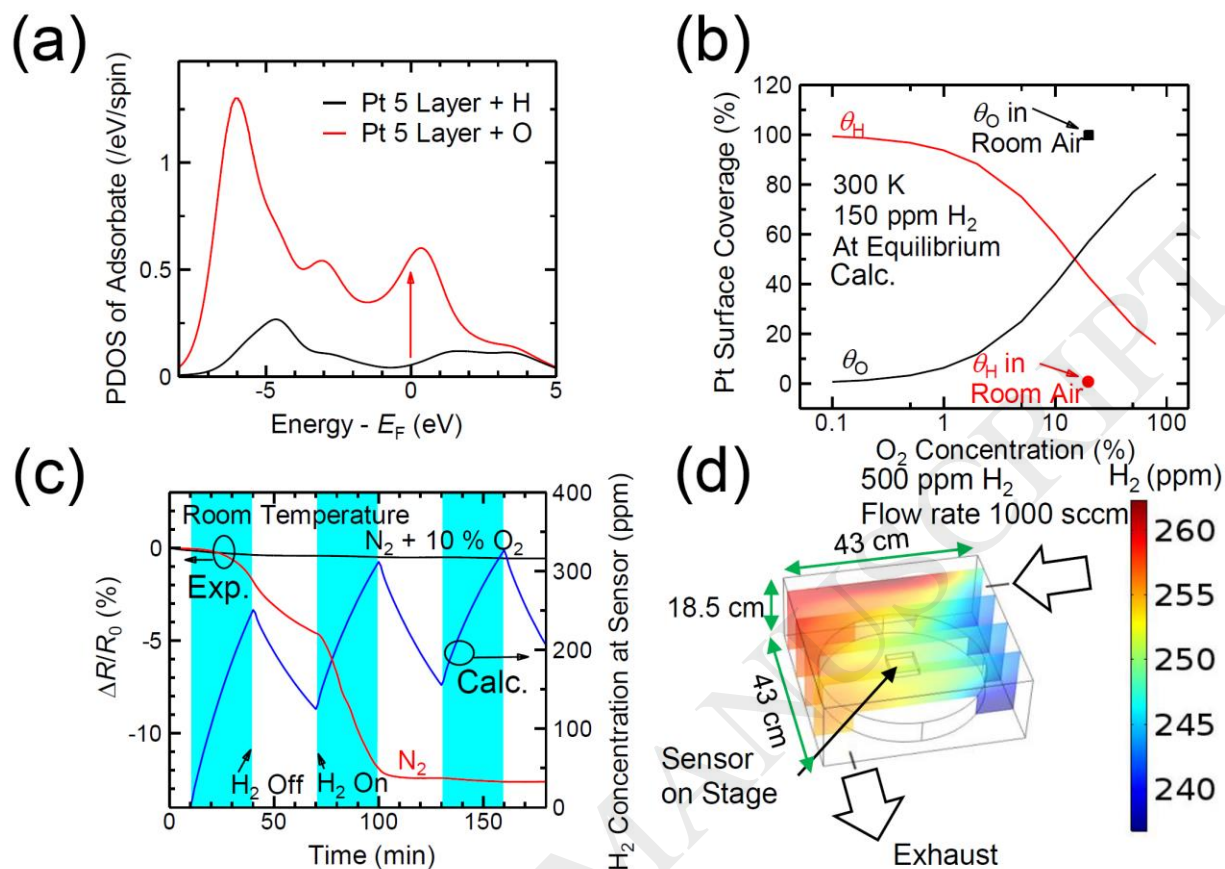


**Fig. 3.** (a) Hydrogen- and oxygen-induced partial density of states for 5 Pt atomic layers. (b) Effects of oxygen concentration on the Pt surface coverage by hydrogen and oxygen atoms. The Pt surface at the room temperature with 150 ppm hydrogen in the atmosphere is assumed. (c) Measured sensor response with and without 10 % oxygen (black and red, respectively), together with the hydrogen concentration at the sensor calculated by COMSOL Multiphysics package (blue). (d) Calculated hydrogen concentration at 150 min in the probe station chamber isolated from room air.



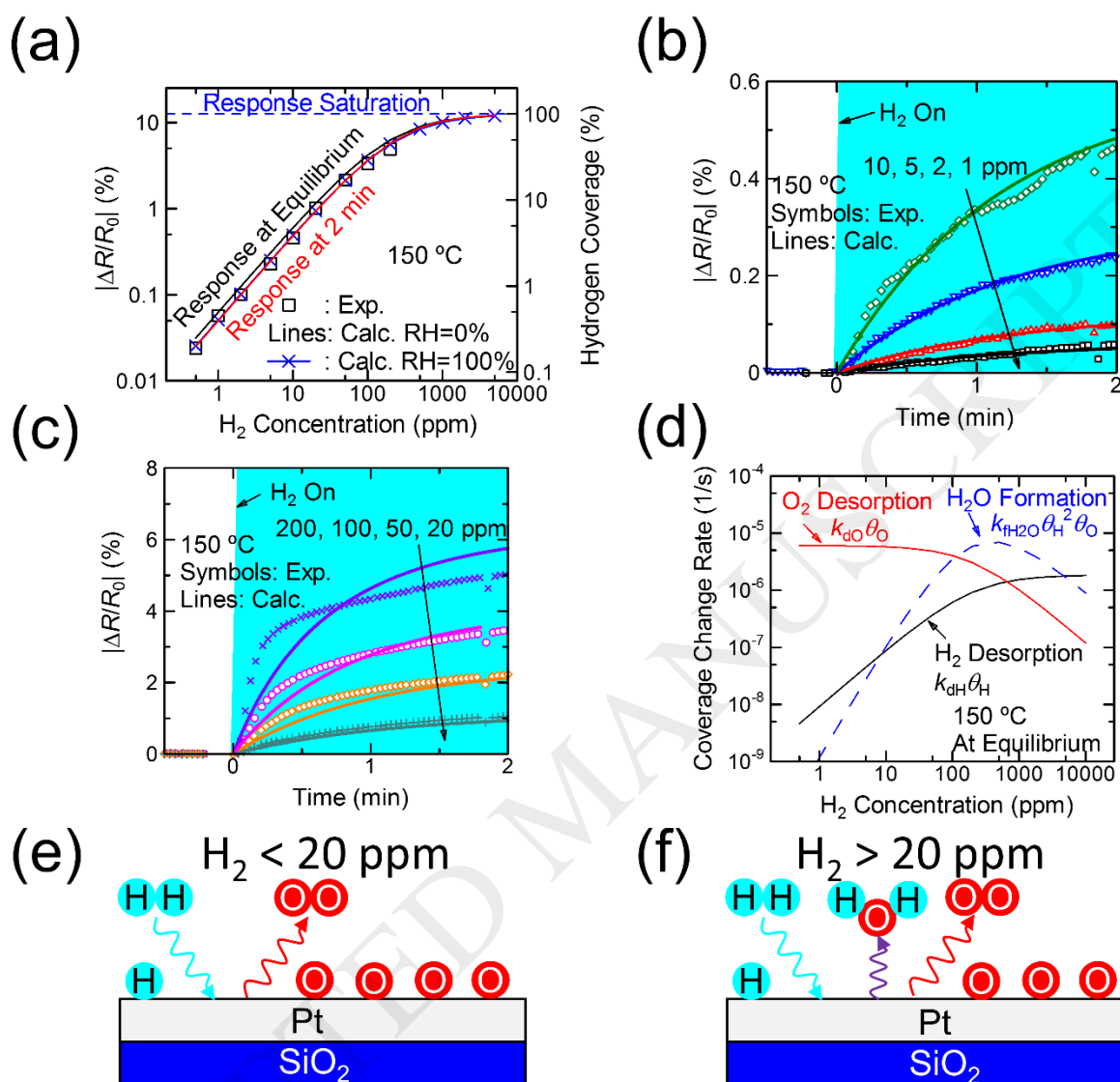


**Fig. 4.** (a) Comparison of the experimental and calculated hydrogen concentration-dependent sensor response at RH = 0 %. The sensor response saturates at 12.6 % when the hydrogen coverage reaches 100 %. Comparison between experimental and calculated time dependence of sensor response at (b) low and (c) high hydrogen concentrations. (d) Hydrogen concentration dependence of the coverage change rate. The values of  $\theta_H$ ,  $\theta_O$ , and  $\theta_{Pt}$  are employed at equilibrium condition. Schematic diagrams of surface reaction at (e) low and (f) high hydrogen concentrations.

<sup>a</sup>The symbols (gas) and (ads) mean the gas phase and adsorbed species, respectively.

## 4. Conclusion

In summary, the sensor response of Pt thin films to hydrogen gas was evaluated through experiments and numerical simulation. By measuring the sensor response under different RH values, both robust sensing against humidity and high sensor response were demonstrated. Furthermore, it was suggested that Pt thin films responded to low-level hydrogen in air expired by a human. The results suggest that these Pt thin films are adequate for detecting hydrogen in expired air, which is characterized by high RH and low hydrogen concentrations. For the first time, a quantitative model was established that relates the hydrogen coverage of the Pt surface to the resistance change, in order to predict the sensor's robustness against humidity and sensor response to hydrogen. The numerically simulated sensor response data are in good agreement with the experimental ones for varying hydrogen concentrations and times, especially at low hydrogen concentration. The hydrogen sensor response derived from experiments and estimated by the proposed model also indicates that these Pt-based hydrogen sensors can be used on expired air.

## Acknowledgement

This work was supported by JST CREST Grant Number JPMJCR1331.

## References

- [1] T. King, M. Elia, J. Hunter, Abnormal colonic fermentation in irritable bowel syndrome, *Lancet*. 352 (1998) 1187–1189. doi:10.1016/S0140-6736(98)02146-1.
- [2] Y. Urita, T. Watanabe, S. Ishihara, T. Maeda, Y. Sasaki, K. Hike, Y. Miura, T. Nanami, K. Arai, H. Koshino, H. Saito, Breath hydrogen and methane levels in a patient with volvulus of the sigmoid colon, *J. Breath Res.* 2 (2008) 37025. doi:10.1088/1752-7155/2/3/037025.
- [3] W. Shin, Medical applications of breath hydrogen measurements, *Anal. Bioanal. Chem.* 406 (2014) 3931–3939. doi:10.1007/s00216-013-7606-6.

- [4] P. Offermans, H.D. Tong, C.J.M. Van Rijn, P. Merken, S.H. Brongersma, M. Crego-Calama, Ultralow-power hydrogen sensing with single palladium nanowires, *Appl. Phys. Lett.* 94 (2009) 223110. doi:10.1063/1.3132064.
- [5] F. Yang, K.C. Donovan, S. Kung, R.M. Penner, The Surface Scattering-Based Detection of Hydrogen in Air Using a Platinum Nanowire, *Nano Lett.* 12 (2012) 2924–2930. doi:10.1021/nl300602m.
- [6] A. Abburi, W.J. Yeh, Temperature and Pore Size Dependence on the Sensitivity of a Hydrogen Sensor Based on Nanoporous Platinum Thin Films, *IEEE Sens. J.* 12 (2012) 2625–2629. doi:10.1109/JSEN.2012.2199298.
- [7] S.H. Lim, B. Radha, J.Y. Chan, M.S.M. Saifullah, G.U. Kulkarni, G.W. Ho, Flexible Palladium-Based H<sub>2</sub> Sensor with Fast Response and Low Leakage Detection by Nanoimprint Lithography, *ACS Appl. Mater. Interfaces.* 5 (2013) 7274–7281. doi:10.1021/am401624r.
- [8] H. Yoo, S. Cho, H. Jeon, H. Jung, Well-Defined and High Resolution Pt Nanowire Arrays for a High Performance Hydrogen Sensor by a Surface Scattering Phenomenon, *Anal. Chem.* 87 (2015) 1480–1484. doi:10.1021/ac504367w.
- [9] S. Takeichi, Y. Ushita, R. Sugai, K. Sakai, T. Kiwa, K. Tsukada, Impedance Evaluation of Hydrogen Sensor Using Ultrathin Platinum Film, *Trans. Mater. Res. Soc. Japan.* 40 (2015) 69–72. doi:10.14723/tmrj.40.69.
- [10] X. Li, Y. Liu, J.C. Hemminger, R.M. Penner, Catalytically Activated Palladium@Platinum Nanowires for Accelerated Hydrogen Gas Detection, *ACS Nano.* 9 (2015) 3215–3225. doi:10.1021/acsnano.5b00302.
- [11] E. Şennik, Ş. Ürdem, M. Erkovan, N. Kilinc, Sputtered platinum thin films for resistive hydrogen sensor application, *Mater. Lett.* 177 (2016) 104–107. doi:10.1016/j.matlet.2016.04.134.

- [12] D. Dwivedi, R. Dwivedi, S.K. Srivastava, Sensing properties of palladium-gate MOS (Pd-MOS) hydrogen sensor-based on plasma grown silicon dioxide, *Sensors Actuators B Chem.* 71 (2000) 161–168. doi:10.1016/S0925-4005(99)00069-6.
- [13] K. Tsukada, T. Kiwa, T. Yamaguchi, S. Migitaka, Y. Goto, K. Yokosawa, A study of fast response characteristics for hydrogen sensing with platinum FET sensor, *Sens. Actuators B.* 114 (2006) 158–163. doi:10.1016/j.snb.2005.04.026.
- [14] A. Spetz, M. Armgarth, I. Lundström, Hydrogen and ammonia response of metal - silicon dioxide - silicon structures with thin platinum gates Hydrogen and ammonia response of metal ... siUcon dioxide-silicon structures with thin platinum gates, *J. Appl. Phys.* 64 (1988) 1274–1283. doi:10.1063/1.341846.
- [15] M. Armgarth, D. Söderberg, I. Lundström, Palladium and platinum gate metal - oxide - semiconductor capacitors in hydrogen and oxygen mixtures, *Appl. Phys. Lett.* 41 (1982) 654–655. doi:10.1063/1.93638.
- [16] T.L. Poteat, B. Lalevic, Pd-MOS hydrogen and hydrocarbon sensor device, *IEEE Electron Device Lett.* 2 (1981) 82–84. doi:10.1109/EDL.1981.25349.
- [17] K. Anand, O. Singh, M.P. Singh, J. Kaur, R.C. Singh, Hydrogen sensor based on graphene/ZnO nanocomposite, *Sensors Actuators B Chem.* 195 (2014) 409–415. doi:10.1016/j.snb.2014.01.029.
- [18] U. Lange, T. Hirsch, V.M. Mirsky, O.S. Wolfbeis, Hydrogen sensor based on a graphene – palladium nanocomposite, *Electrochim. Acta.* 56 (2011) 3707–3712. doi:10.1016/j.electacta.2010.10.078.
- [19] B. Hwan, C.F. Lo, J. Nicolosi, C.Y. Chang, V. Chen, W. Strupinski, S.J. Pearton, F. Ren, Hydrogen detection using platinum coated graphene grown on SiC, *Sens. Actuators B.* 157 (2011) 500–503. doi:10.1016/j.snb.2011.05.007.

- [20] W. Wu, Z. Liu, L.A. Jauregui, Q. Yu, R. Pillai, H. Cao, J. Bao, Y.P. Chen, S. Pei, Sensors and Actuators B : Chemical Wafer-scale synthesis of graphene by chemical vapor deposition and its application in hydrogen sensing, *Sens. Actuators B.* 150 (2010) 296–300. doi:10.1016/j.snb.2010.06.070.
- [21] L. Al-Mashat, K. Shin, K. Kalantar-zadeh, J.D. Plessis, S.H. Han, R.W. Kojima, R.B. Kaner, D. Li, X. Gou, S.J. Ippolito, W. Wlodarski, Graphene/Polyaniline Nanocomposite for Hydrogen Sensing, *J. Phys. Chem. C.* 114 (2010) 16168–16173. doi:10.1021/jp103134u.
- [22] A. Kaniyoor, R.I. Jafri, T. Arockiadoss, S. Ramaprabhu, Nanostructured Pt decorated graphene and multi walled carbon nanotube based room temperature hydrogen gas sensor, *Nanoscale.* 1 (2009) 382–386. doi:10.1039/b9nr00015a.
- [23] J. Kong, M.G. Chapline, H. Dai, Functionalized Carbon Nanotubes for Molecular Hydrogen Sensors, *Adv. Mater.* 13 (2001) 1384–1386. doi:10.1002/1521-4095(200109)13:18<1384::AID-ADMA1384>3.0.CO;2-8.
- [24] Z. Zhao, M. Knight, S. Kumar, E.T. Eisenbraun, M.A. Carpenter, Humidity effects on Pd / Au-based all-optical hydrogen sensors, *Sens. Actuators B.* 129 (2008) 726–733. doi:10.1016/j.snb.2007.09.032.
- [25] P. Giannozzi, S. Baroni, N. Bonini, M. Calandra, R. Car, C. Cavazzoni, D. Ceresoli, G.L. Chiarotti, M. Cococcioni, I. Dabo, A.D. Corso, S. De Gironcoli, S. Fabris, G. Fratesi, R. Gebauer, U. Gerstmann, C. Gougoussis, A. Kokalj, A. Gulans, S. Kontur, C. Meisenbichler, C. Friedrich, M. Betzinger, M. Schlipf, P. Giannozzi, S. Baroni, N. Bonini, M. Calandra, R. Car, C. Cavazzoni, D. Ceresoli, G.L. Chiarotti, M. Cococcioni, I. Dabo, A.D. Corso, S. De Gironcoli, U. Gerstmann, C. Gougoussis, A. Kokalj, M. Lazzeri, L. Martin-Samos, N. Marzari, F. Mauri, R. Mazzarello, S. Paolini, A. Pasquarello, L. Paulatto, C. Sbraccia, S. Scandolo, G. Sclauzero, S.A. P. A. Smogunov, P. Umari, R.M. Wentzcovitch, QUANTUM ESPRESSO : a modular and open-source software project for quantum

- simulations of materials, *J. Phys. Condens. Mat.* 21 (2009) 395502. doi:10.1088/0953-8984/21/39/395502.
- [26] J.P. Perdew, J.A. Chevary, S.H. Vosko, K.A. Jackson, M.R. Pederson, D.J. Singh, C. Fiolhais, Atoms, molecules, solids, and surfaces: Applications of the generalized gradient approximation for exchange and correlation, *Phys. Rev. B.* 46 (1992) 6671–6687. doi:10.1103/PhysRevB.46.6671.
- [27] F. Liu, C. Wu, G. Yang, S. Yang, CO Oxidation over Strained Pt(100) Surface: A DFT Study, *J. Phys. Chem. C.* 119 (2015) 15500–15505. doi:10.1021/acs.jpcc.5b04511.
- [28] W.R. Williams, C.M. Marks, L.D. Schmidt, Steps in the reaction hydrogen + oxygen .dblharw. water on platinum: hydroxy desorption at high temperatures, *J. Phys. Chem.* 96 (1992) 5922–5931. doi:10.1021/j100193a051.
- [29] J.L. Gland, B.A. Sexton, G.B. Fisher, Oxygen interactions with the Pt(111) surface, *Surf. Sci.* 95 (1980) 587–602. doi:10.1016/0039-6028(80)90197-1.
- [30] U. SCHMIDT, Molecular hydrogen in the atmosphere, *Tellus.* 26 (1974) 78–90. doi:10.1111/j.2153-3490.1974.tb01954.x.
- [31] M. Nishibori, W. Shin, N. Izu, T. Itoh, I. Matsubara, Sensing performance of thermoelectric hydrogen sensor for breath hydrogen analysis, *Sensors Actuators, B Chem.* 137 (2009) 524–528. doi:10.1016/j.snb.2009.01.029.
- [32] Y. Kondo, T. Liu, F. Toda, Milk is a useful test meal for measurement of small bowel transit time, *J. Gastroenterol.* 29 (1994) 715–720. doi:10.1007/BF02349276.
- [33] A. Shimouchi, K. Nose, M. Yamaguchi, H. Ishiguro, T. Kondo, Breath hydrogen produced by ingestion of commercial hydrogen water and milk., *Biomark. Insights.* 4 (2009) 27–32. <http://www.pubmedcentral.nih.gov/articlerender.fcgi?artid=2716677&tool=pmcentrez&rendertype=abstract>.

- [34] R.G. Tobin, Mechanisms of adsorbate-induced surface resistivity??experimental and theoretical developments, *Surf. Sci.* 502–503 (2002) 374–387. doi:10.1016/S0039-6028(01)01978-1.
- [35] P. Wissmann, The effect of gas adsorption on the conductivity of thin metal films, *Thin Solid Films.* 13 (1972) 189–193. doi:10.1016/0040-6090(72)90173-3.
- [36] B. HELLSING, Kinetics of the hydrogen-oxygen reaction on platinum, *J. Catal.* 132 (1991) 210–228. doi:10.1016/0021-9517(91)90258-6.
- [37] G. Fischer, H. Hoffmann, J. Vancea, Mean free path and density of conductance electrons in platinum determined by the size effect in extremely thin films, *Phys. Rev. B.* 22 (1980) 6065–6073. doi:10.1103/PhysRevB.22.6065.
- [38] J. Vancea, H. Hoffmann, K. Kastner, Mean free path and effective density of conduction electrons in polycrystalline metal films, *Thin Solid Films.* 121 (1984) 201–216. doi:10.1016/0040-6090(84)90302-X.

## Author Biographies

**Takahisa Tanaka** received his B. Eng., and M. Eng., and Dr., Eng. degrees from Keio University in 2010, 2012, and 2015. He has been an assistant professor at Keio University since 2016. His current research interest are characterizations of nanostructured materials applied to LSI and sensors.

**Shisuke Hoshino** received his M. Eng., degrees from Keio University in 2016. His research interest is change in resistance of metal thin films by hydrogen.

**Tsunaki Takahashi** received the B. Eng., M. Eng., and Dr. Eng. degrees in electrical engineering from Tokyo Institute of Technology in 2009, 2011, and 2013, respectively. He is currently a research assistant professor in institute for materials chemistry and engineering at Kyushu University. His primary research interests are in the area of thermal properties in nanoscale electron devices and molecular recognition sensor devices based on metal oxide and/or silicon nanotechnology.

**Ken Uchida** received B.S. degree in physics, M.S. and Ph.D. degrees in applied physics all from the University of Tokyo, Tokyo, Japan, in 1993, 1995, and 2002, respectively. In 1995, he joined the Research and Development Center, Toshiba Corporation, Kawasaki, Japan. He has studied carrier

transport in nanoscale devices such as Single-Electron Devices, Schottky source/drain MOSFETs, Ultrathin-body SOI MOSFETs, Strained Silicon MOSFETs, Carbon Nanotube Transistors, and (110) Si MOSFETs. In 2008, he moved to Tokyo Institute of Technology, Tokyo, Japan, as an associate professor, where he worked on properties of shallow impurities and thermal transport in nanoscaled silicon. In 2012, he moved to Keio University, Yokohama, Japan, as a full professor.

**Table 1.** Adsorption and desorption kinetic parameters on Pt.

index	reaction <sup>a</sup>	pre-exponential or sticking coefficient (s <sup>-1</sup> )	activation energy (kcal/mol)
	H <sub>2</sub> (gas)→2H(ads)	0.5	0.0
dH	2H(ads)→H <sub>2</sub> (gas)	4.0×10 <sup>4</sup>	20.0
	O <sub>2</sub> (gas)→2O(ads)	0.002	0.0
dO	2O(ads)→O <sub>2</sub> (gas)	4.0×10 <sup>4</sup>	19.0
	H <sub>2</sub> O(gas)→ H <sub>2</sub> O (ads)	0.002	0.0
dH <sub>2</sub> O	H <sub>2</sub> O(ads)→ H <sub>2</sub> O (gas)	4.0×10 <sup>4</sup>	10.0